Materials and Design 204 (2021) 109622

Contents lists available at ScienceDirect

Materials and Design

journal homepage: www.elsevier.com/locate/matdes

Assembly-induced microwave band resonance in gold nanoparticles-based ultrathin and flexible spoof localized surface plasmon

Peng Wang [a,b], Xiaopeng Shen [c], Haochi Zhang [d], Ou Xu [d], Peihang He [d], Haoshen Wang [c], Siyu Ma [a,e], Zhaobin Guo [f], Qing Jiang [b], Ning Gu [a,*], Jianfei Sun [a,*]

[a] State Key Laboratory of Bioelectronics, Jiangsu Key Laboratory for Biomaterials and Devices, School of Biological Science and Medical Engineering, Southeast University, Nanjing 210009, PR China
[b] Department of Sports Medicine and Adult Reconstructive Surgery, Drum Tower Hospital affiliated to Medical School of Nanjing University, Zhongshan Road 321, Nanjing 210008, PR China
[c] Department of Physics, China University of Mining and Technology, Xuzhou 221116, PR China
[d] State Key Laboratory of Millimetre Waves, Department of Radio Engineering Southeast University, Nanjing 210096, PR China
[e] Drum Tower Hospital affiliated to Nanjing University Medical School, Nanjing, Jiangsu 210008, China
[f] Institute for Nanobiotechnology, Johns Hopkins University, Baltimore, MD, United States

HIGHLIGHTS

- Ultrathin and flexible spoof localized surface plasmon is fabricated by LBL assembly of gold nanoparticles.
- The spoof localized surface plasmon exhibits assembly-induced LSPR resonance in microwave band.
- Disappearance of electric resonance component resulting in high surface impedance.
- Strong relationship between resonance frequency and curvature degree was observed.

GRAPHICAL ABSTRACT

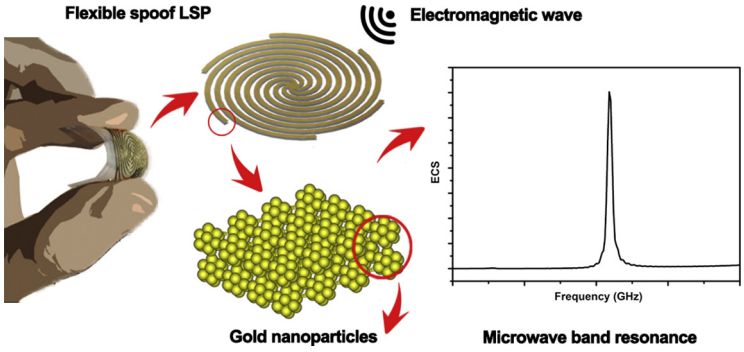

ARTICLE INFO

Article history:
Received 10 November 2020
Received in revised form 25 February 2021
Accepted 27 February 2021
Available online 3 March 2021

Keywords:
Spoof LSP
Optical/microwave dual bands
Layer-by-layer assembly
Gold nanoparticles

ABSTRACT

Spoof LSP (Localized Surface Plasmon) is a great advance in metamaterials, expanding the LSP resonance from optical band into microwave band. It will yield amazing outcomes by integration with flexible electronics, wearable electronics and nanophotonics. Here, an ultrathin and flexible spoof LSP prepared by layer-by-layer (LBL) assembly of gold nanoparticles was demonstrated. The LSPR effects in microwave band was assembly-induced and the electric resonance component disappeared, which is significantly different from that of the spoof LSPs by bulk metal. It was thought and proved by simulation to be relative with the special micro-structure of the gold nanoparticle assemblies. Furthermore, the spoof LSP by gold nanoparticles was flexible and showed a strong relationship between the resonance frequency and the curvature degree of the spoof LSP, meaning that the LSP resonance can be modulated by the deformation of the spoof LSP. We believed that these results could deepen understanding about the spoof LSPs and widen the application in multiple areas.

* Corresponding authors at: State Key Laboratory of Bioelectronics, Jiangsu Key Laboratory for Biomaterials and Devices, School of Biological Science and Medical Engineering, Southeast University, Nanjing 210009, PR China.
E-mail addresses: guning@seu.edu.cn (N. Gu), sunzaghi@seu.edu.cn (J. Sun).

https://doi.org/10.1016/j.matdes.2021.109622

1. Introduction

Localized surface plasmon (LSP) resonance is an important phenomenon in physics and has extensive applicability in practice. [1–3] Noble metal nanoparticles are elemental units for this effect in optical band, based on which, emerging nano-photonics have shown greatly promising to essentially change the state of art in ultra-sensitive detection [4,5], near-field optics [6,7] and optoelectronics [8,9]. Recently, some metamaterials with specific structure have been discovered to have the similar performance in microwave band, which were called spoof LSPs [10,11]. The spoof LSPs can realize the control of microwave by the artificial structure at subwavelength scale rather than by the composition of materials. With the spoof LSPs, the photonics-based applications can be facilely grafted into the microwave range, which brings about advantages of deeper penetration depth [12], larger acting scale [13] and better capability of anti-interference. [14] Therefore, our idea is to integrate the two resonance effects into one device by fabricating the spoof LSPs with noble metal nanoparticles. This "two-in-one" strategy may mediate fantastic interactions between the light and the microwave, possibly bringing about some innovative applications. Meanwhile, the composition of nanoparticles will confer the flexibility on the spoof LSPs, [15,16] complementing some drawbacks of the current PCB (printed circuit board) in technics. With this innovation, metamaterials will greatly widen the application in flexible electronics. [17] Therefore, it is primary and greatly necessary to investigate microwave responses of the flexible spoof LSPs which were fabricated by assembly of numerous metal nanoparticles.

Gold nanoparticles are one important type of noble metal nanomaterials, which are considered well biocompatible and possess tailorable optical properties resulting from the LSPR effect. [18–20] Gold nanoparticles had been the elemental units in single-electron devices, which showed promising prospect in quantum logic operations, storage and sensing. [21] Moreover, the thiolated DNA functionalized gold nanoparticles can also be used as building blocks to establish multifunctional two-dimensional gold assembled films through the sequence specific interaction of DNA [22]. Chen and *co*-workers reported the Plasmonic superlattice membrane fabricated by polymer-ligand-based strategy in drying-mediated self-assembly at the air/water interfaces [23]. Recently, with development of wearable devices, researchers also pay increasing attentions to the assemblies of Gold nanoparticles, such as the stretchable and bendable two-dimensional (2D) film. [24,25] Furthermore, the freestanding LBL film of gold nanoparticles can be obtained when the assembled layer exceed 500 and the as-prepared film was also flexible and could be used as flexible conductors [26]. During our previous studies, we found the 2D LBL-assembled film of gold nanoparticles exhibited a transition from insultor into conductor tailored by the assembled density. [27] This phenomenon was thought to result from the assembly-induced shift of energy absorption cross-section from the optical band into the low frequency range. Thus, it is feasible to fabricate the spoof LSPs by the assembly of Gold nanoparticles, possibly exhibiting the LSPR in optical/microwave dual bands.

In this work, an ultrathin and flexible spoof LSP by layer-by-layer (LBL) assembly of gold nanoparticles was firstly prepared. LSPR resonance of spoof LSPs with vairous assembled layers in microwave band were comprehensively investigated using vector network analyzer, near-field distributions measurement and resonance simulation. The spoof LSPs fabricated by bulk metal were used as control. Surprisingly, the electric resonance component disappeared, which is significantly different from that of the spoof LSPs by bulk metal. After simulation and experimental investigations, the surface impedance of spoof LSP have great influence on their resonance signal and the disappearance of the electric LSPs resonance mode may be due to their high surface impedance. Furthermore, the spoof LSP by gold nanoparticles was flexible and showed a strong relationship between the resonance frequency and the curvature degree of the spoof LSP. It's known that the human tissue can be effectively penetrated by electromagnetic field, the ultrathin and flexible spoof LSP LBL-assembled by gold nanoparticles with optical/microwave resonance band will attract considerable attention in application of multiple areas.

2. Materials and methods

2.1. Synthesis of gold nanoparticles

The citrate-capped gold nanoparticles were synthesized according to a previously reported method using classical citrate reduction method [28]. Briefly, 96 mL of $HAuCl_4 \cdot 3H_2O$ (0.25 mM) was added to a 250 mL three-necked round-bottomed flask equipped with mechanical stir bar. The solution was heated until boiling. Subsequently, 4 mL 1% (weight/volume) trisodium citrate was added to the solution. The mixture solution was heated for 25 min until the colour of solution firstly turned to red and then cooled down to room temperature. Specifically, condensing plant was in working state all through the progress. To prepare the dipping solution for LBL films, as-prepared aqueous solution needs to be concentrated to 10% by centrifuging at 10300 rpm for 33 min.

2.2. Layer-by-layer assembly of spoof LSP

The ITO substrate was firstly machined to the spiral structure by laser beam cutting method. Before the progress of assembly, the spiral ITO substrate was modified by plasma surface treatment to make the surface charged. Then the charged spiral ITO substrate was dipped into 2% (weight/volume) Poly-diallyldimethylammonium Chloride (PDDA) solution for 10 min. After being washed by deionized water and dried by nitrogen gas, the substrate was dipped into the as-prepared concentrated colloidal gold for 15 min, cleaned and dried again as above, thus achieving 1 layer Gold NPs Film. The ultrathin and flexible spoof LSP was obtained by the 40 times repeating of the process.

2.3. Simulation

The resonance simulation of spoof LSP is performed by the commercial software, CST Microwave Studio 2016. The metal (Au, Ag and Cu) is selected in the material library in CST. For ECS calculation, a plane-wave excitation is applied across the surface of spoof LSP and a broadband far-field monitor is employed to record the scattering cross sections. Based on the CST eigenmode solver, the calculation of dispersion relation is analyzed. The simulation for electromagnetic response of the imitative LBL-assembled film of gold nanoparticles is used by the commercial software, Comsol Multiphysics 5.6. The structures of the film that consist of Au clusters were assigned as a domain of which material is gold and the environment was set as air whose refractive index is 1.003. The coming plane electromagnetic wave, the frequency of which was set as 2 GHz, was propagated along the surface of the imitative LBL-assembled film. The electromagnetic response form was solved using the finite element method.

2.4. Resonance measurement of the flexible spoof LSP

The ultrathin and flexible spoof LSP was firstly attached to the side wall of nylon cylinder with different bottom radius. Then the 30–300 angle bent spoof LSP was measured by vector network analyzer, the process of which was carried out as following: the electromagnetic wave was launched at 45 degree incident angle across the spoof LSP from the source monopole antenna to the monopole probe, the resonance signal of which was obtained by vector network analyzer.

2.5. Near-field distributions measurement

The Near-field distributions of spoof LSP was measured using a 3D Near-field scanning platform. A plane wave caused by ultra-wide band antenna was used as signal source and the spoof LSP was placed in

front of the antenna. The monopole probe was placed above the surface of spoof LSP with the distance of 5 mm. Both the ultra-wide band antenna and the monopole probe were connected to the vector network analyzer. The ultra-wide band antenna and the spoof LSP are placed on a mechanical platform that can move in a horizontal scan direction. The near-field distributions can be measured and drew as 2D image where the gradient colour represent the different intensity.

2.6. Characterizations

The optical property of gold nanoparticles was measured using a UV–vis Spectrophotometer (Shimadzu, UV-3600, Japan). The morphology of assembled metamaterial was observed by field emission scanning electron microscope (Zeiss Supra 40 Gemini, Germany), transmission electron microscopy (TEM, JEM-2100, Japan) and atomic force microscopy (AFM, 5500AFM/STM, China). The ITO substrate of the spoof LSP was machined by laser beam cutting machine (LPKF Laser & Electronics, China). The resonance property of LBL-assembled gold NPs spoof LSP was measured by vector network analyzer (Keysight-E5063A). The surface impedance of spoof LSP from 1 MHz to 3GHz was meaured using a high-frequency impedance analyzer (Keysight, E4991B)

3. Results and discussion

Structure of the spoof LSP in this work was schematically shown in Fig. 1a, which was consisted of a metallic disk with radius 0.4 mm and six spiral arms. The spiral geometry can be parametrized as

$$\begin{aligned} x &= (d + at)\cos(t) \\ y &= (d + at)\sin(t) \end{aligned} \tag{1}$$

where t is intersection angle of spiral line, a is intersection growth rate and d is the distance between initial point of spiral line and origin of coordinates. The spiral geometry in our study is built with 60°intersection angle for 6 times. Both width of the arms and distance between the two arms were 0.4 mm. Radius of the whole structure was 9.5 mm. This structure was reported to have dual peaks in the microwave band where one is corresponding to electric resonance component and the other to magnetic resonance component [14,29,30]. The electromagnetic properties of spoof LSP was firstly theoretical calculated using a reported analytical model [31]. In order to simplify calculating, the refractive index of dielectric material was given by 1. When TM waves horizontally propagated across the spiral structure, spoof LSP can be excited and the analytical form of Hz can be found as:

$$H_z \begin{cases} \sum_{n=-\infty}^{\infty} \left[i^n J_n(k_0\rho) + b_n H_n^{(1)}(k_0\rho) \right] e^{in\psi} & \rho \geq R \\ \sum_{n=-\infty}^{\infty} [c_n J_0(k_0\rho) + d_n Y_0(k_0\rho)] e^{in\psi} & R \geq \rho \geq r \end{cases} \tag{2}$$

Where ρ is radial distance, J_n is Bessel function, Y_n is Neumann function, $H_n^{(1)}$ is Hankel function of the first kind. Applying the boundary conditions ($\rho = R$):

$$i^n J_n(k_0\rho) + b_n H_n^{(1)}(k_0\rho) = c_n J_0(k_0\rho) + d_n Y_0(k_0 R) \tag{3}$$

$$i^n J_n'(k_0\rho) + b_n H_n^{(1)'}(k_0\rho) = -\frac{m}{n}[c_n J_1(k_0\rho) + d_n Y_1(k_0 R)] \tag{4}$$

$$c_n J_1(k_0 r) + d_n Y_1(k_0 r) = 0 \tag{5}$$

After Hz was obtained, the scattering cross section σ of spoof LSP can be obtained accodring to the Mie theory [32]:

$$\sigma = \frac{4}{k_0} \sum_{n=-\infty}^{\infty} |b_n|^2 \tag{6}$$

where bn is the scattering coefficient of the nth-order spiral structure. It takes the form

$$b_n = -i^n \frac{\frac{m}{n} J_n(k_0 R) f - J_n'(k_0 R) g}{\frac{m}{n} H_n^{(1)}(k_0 R) f - H_n^{(1)'}(k_0 R) g} \tag{7}$$

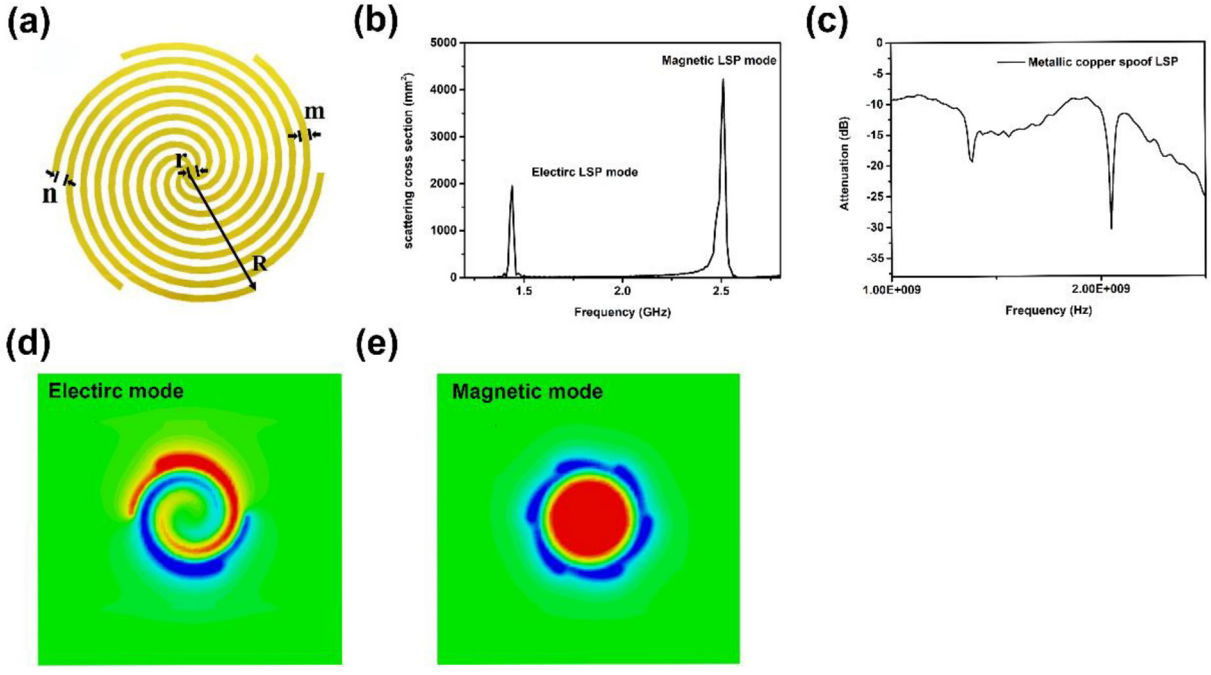

Fig. 1. The spoof LSP of bulk Cu with spiral structure. a) Schematic structure of the spiral spoof LSP. b) Simulation of the extinction cross section of spiral spoof LSP by CST software. c) Experimental measurement of LSP resonance for the spiral spoof LSP made up of metallic copper. d) and e) Simulated results of the electric resonance mode and the magnetic resonance mode, respectively. The observation plane was set 0.5 mm above the surface of spiral.

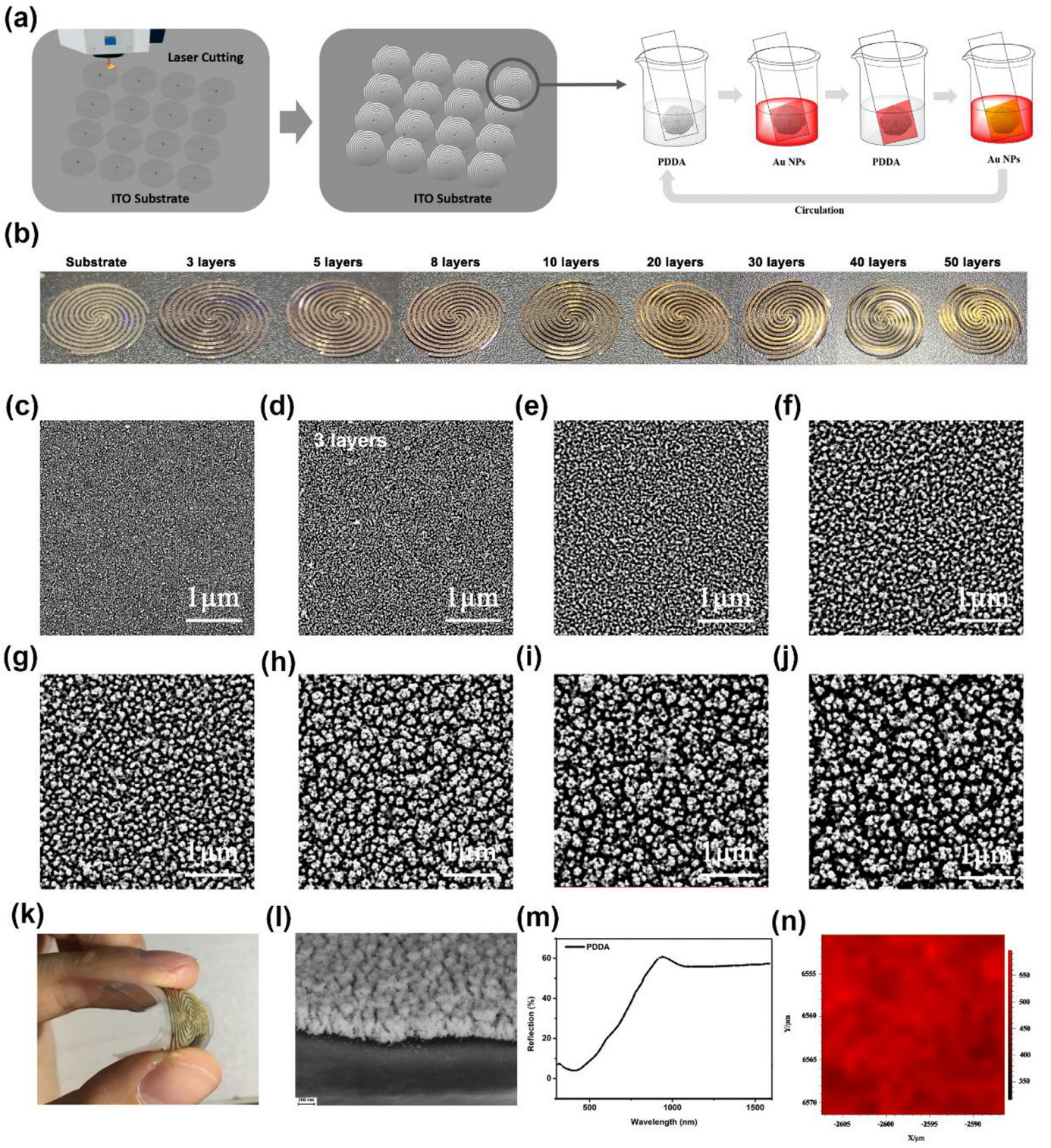

Fig. 2. The spoof LSP with the same spiral structure fabricated by assembly of Au nanoparticles. a) Schematic show of the process to fabricate the ultrathin and flexible spoof LSP on ITO substrate by LBL-assembly of Au nanoparticles. b) Photographs of the assembled spiral spoof LSP with 3, 5, 8, 10, 20, 30, 40, 50 layers, respectively. c-j) TEM of as-prepared assembled spiral spoof LSP with 3, 5, 8, 10, 20, 30, 40, 50 layers, respectively. k) Flexibility show of the spoof LSP. l) SEM image of the cross-section for the spiral. m) UV–Vis reflectance spectrum of the spoof LSP. n) Raman mapping of the spoof LSP.

$$f = J_1(k_0r)Y_1(k_0R) - J_2(k_0R)Y_1(k_0r) \quad (8)$$

$$g = J_0(k_0R)Y_1(k_0r) - J_1(k_0r)Y_1(k_0R) \quad (9)$$

In addition, extinction cross section of this spoof LSP was calculated in the case that a plane wave propagated across its surface by using CST software (Fig. 1b). It was theoretically predicted that there are two resonance peaks at 1.45 GHz and 2.5 GHz, respectively. It is well-accepted that bulk Au is not recommended for use due to its high cost with PCB technics while the fabrication of Cu spiral structure is cheap and mature. Thus, we chose the bulk Cu spoof LSP for experimental study, the result of which was confirmed with vector network analyzer (Fig. 1c),

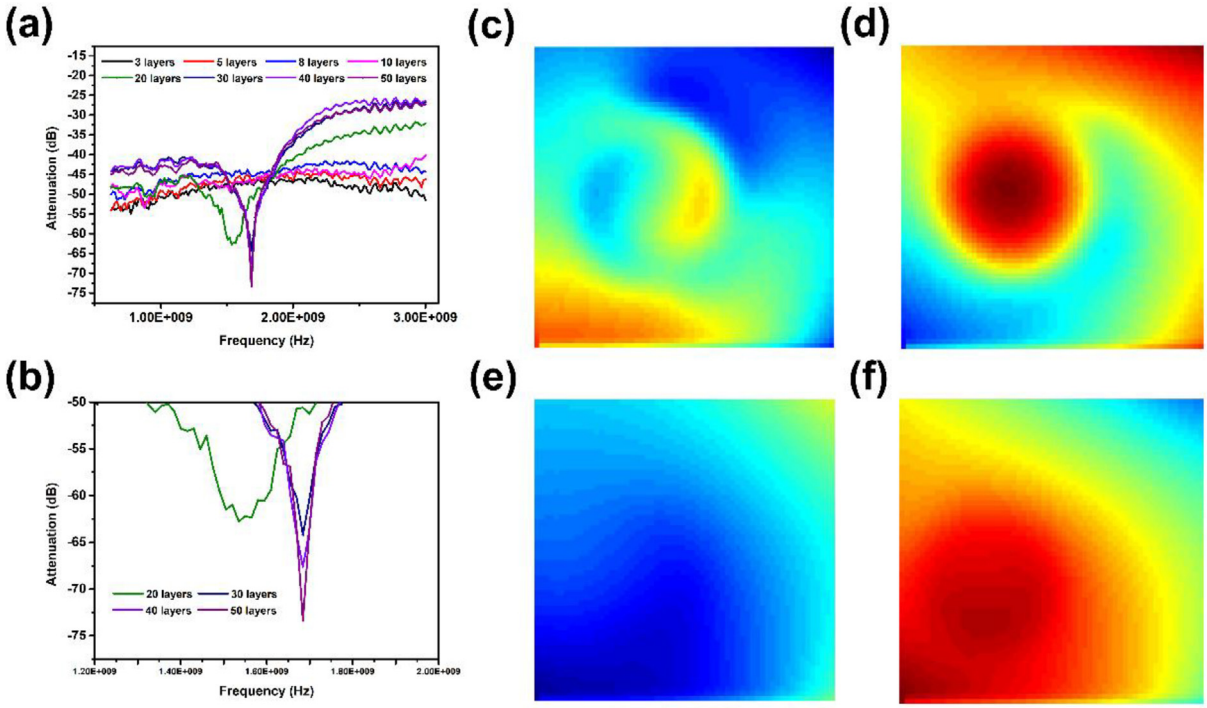

Fig. 3. LSP resonance investigation of the spoof LSP fabricated by assembly of Au nanoparticles. a) LSP resonance measurements of the assembled spiral spoof LSP with 3, 5, 8, 10, 20, 30, 40, 50 layers, respectively. b) Local magnification for the LSP resonance measurements of the assembled spiral spoof LSP with 20, 30, 40, 50 layers, respectively. c) and d) Experimental measurements of near field distribution of the electric resonance mode and the magnetic resonance mode for the spoof LSP of bulk copper, respectively. The observation plane was set 0.5 mm above the surface of spoof LSP. e) and f) Experimental measurements of near field distribution of the electric and the magnetic resonance modes for the spoof LSP by assembly of Au nanoparticles, respectively. The observation plane was set 0.5 mm above the surface of spoof LSP.

showing two peaks at 1.38 GHz and 2.05 GHz. The simulated distributions of electric field (Fig. 1d, e) indicated that the two peaks at 1.45 GHz and 2.5 GHz represent the electric and the magnetic resonance modes, respectively.

We firstly synthesized the citrate-capped gold nanoparticles which showed relative narrow size dispersity (Supplementary Information, Fig. S1). The average diameter was about 17.98 ± 0.84 nm. The diameter distribution result was measured by a particle size analysis software, where the diameter of each particle in TEM image can be hand-actuated measured according to the scale bar and the average diameter of all measured nanoparticles can be calculated automatically. UV–Vis spectra confirmed the high reproducibility of the nanoparticles synthesized from different batches, which guaranteed the uniformity and reproducibility of assembled films (Supplementary Information, Fig. S2). The relative uniform of the gold nanoparticle we as-preapred could be used as building blocks to construct two-dimension assembled film of gold nanoparticles, which was in accordance with the work in Kotov's work [33]. LBL assembly was a facile and versatile dip-coating method to controllably construct multifunctional film, where polyelectrolyte PDDA was widely used as polymeric partner for assembly of metal nanoparticles [34]. The gold nanoparticles are negatively charged due to the surface modification of citrate and PDDA are positively charged, allowing us to use LBL method to obtain assembly film of gold nanoparticles. In addition, the high concentration of reactant (gold nanoparticles and PDDA) can provide more initial adsorption potential, guaranteeing the successful process of LBL assembly [35]. The ultrathin and flexible spoof LSPs were fabricated by the LBL assembly of gold nanoparticles on ITO film that was pre-cut into the spiral structure as the spoof LSP by laser beam cutting method, as schematically shown in Fig. 2a. It should be mentioned that the ITO layer was under the assembled spoof LSP and the ITO film was bought from the company (Xiaocheng, China), whose sheet impedance and thickness were 6 $\Omega \cdot cm^2$ and 0.125 mm respectively. Photographs of the assembled spiral LSP from 3 layers to 50 layers was present in Fig. 2b, which showed a gradually metal-like appearance with the assembled layer increased. Low magnification scanning electron microscope (SEM) images of typical assembled LSP (Supplementary Information, Fig. S3) showed that the surface was comparative smooth, indicating the high reproducibility and uniformity of LBL assembly of gold nanoparticles. High-magnification SEM images were shown in Fig. 2c-j, where it can be seen that the gold nanoparticles formed clusters with size about 100 nm and the LSP device was built by the accretion of the clusters, which became larger and larger with added layer numbers. And this result was confirmed by atomic force microscopy (AFM) (Supplementary Information, Fig. S4). Furthermore, it was flexible (Fig. 2k). Based on our previous results, the film of gold nanoparticles will turn highly conductive after 30 layers assembly. Seen from the SEM images of cross section (Fig. 2l), the thickness of the LSP device for 30 layers of LBL-assembly was 221.2 nm that is obviously much smaller than the wavelength of microwave.

The optical resonance was further measured. The far-field absorption spectrum of spoof LSP LBL-assembled on silicon wafer was shown in Fig. 2m. The LSPR peak was also observed but the width turned greatly broadened and the resonance wavelength shifted to 400 nm while that of the monodispersed gold nanoparticles was in 520 nm. This phenomenon is because of the strong electromagnetic couplings resulting from aggregation of the gold nanoparticles [36,37]. The near-field Raman mapping was shown in Fig. 2n. It was manifested that the Raman signals were fairly uniform, which rooted in the uniformity of gold nanoparticles assembly. Based on the intensity bar, the enhancement factor of the assembled film approximated 1000. This value is not extremely high for Raman enhancement, but it meant the uniform and compact film of gold nanoparticles still preserved the near field optical effect from the LSPR property of gold nanoparticles.

Then the LSPR effect of the ultrathin and flexible spiral LSP with 3 layers to 50 layers of LBL assembly of gold nanoparticles in microwave band was measured with vector network analyzer. Firstly, influence upon the resonance signal was ruled out from the spiral substrate (ITO

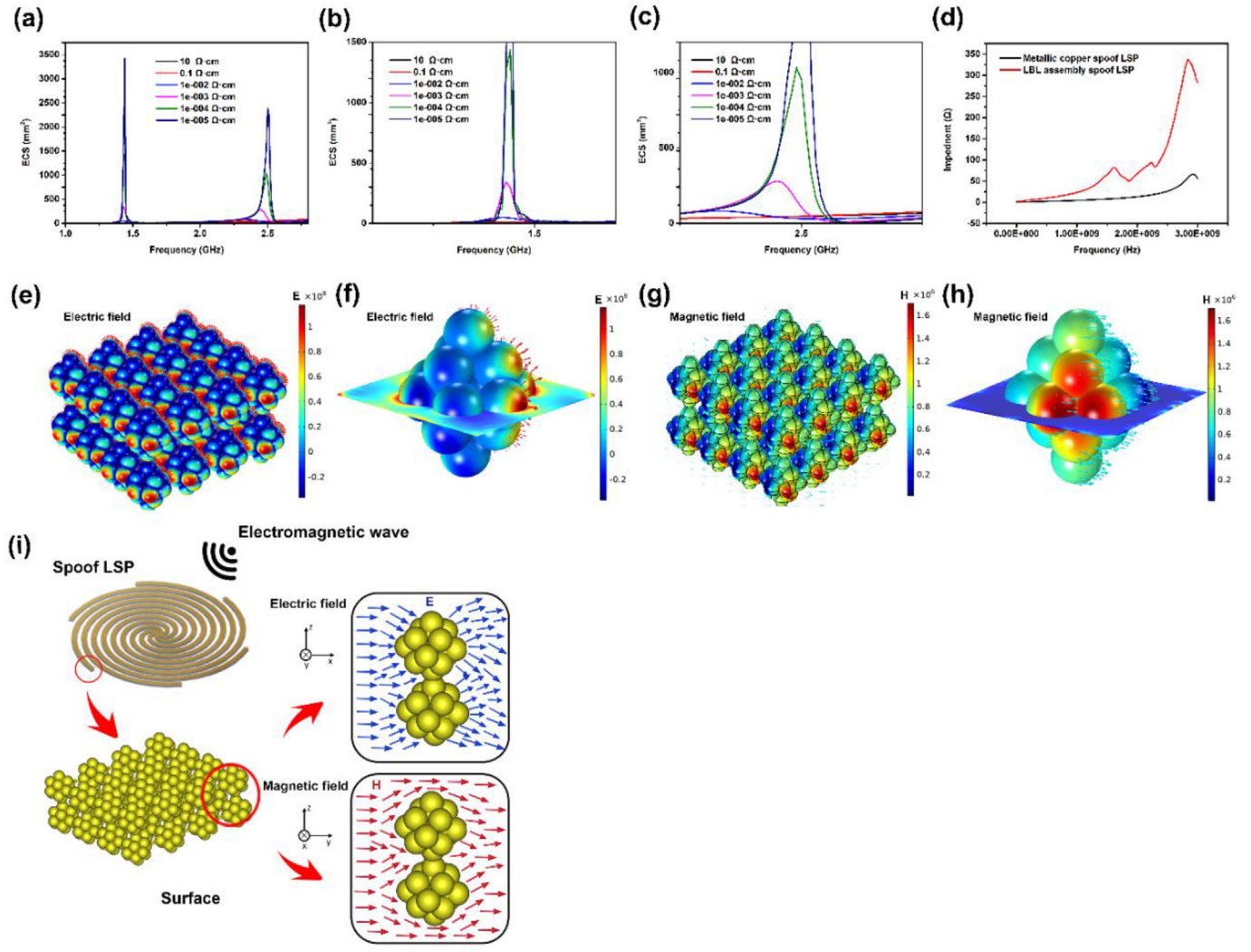

Fig. 4. Influence from the structure of the spoof LSP by assembly of Au nanoparticles upon the LSP resonance. a) Simulated LSPR spectra of the spiral spoof LSP with various surface impedance by CST software. The spiral spoof LSP was set as bulk metal. b) and c) Local magnification for the electric resonance mode and the magnetic electric resonance mode in a). d) Experimental measurement results of surface impedance for the bulk copper and the assemblies of Au nanoparticles from 1 MHz to 3GHz by high-frequency vector network analyzer. e-f) Simulated surface electric field distribution and local magnification of assembled films by Au clusters by COMSOL software. g-h) Simulated surface magnetic field distribution and local magnification of assembled films by Au clusters by COMSOL software. h) Scheme of the possible mechanism for the LSPR spectrum of the spoof LSP by assembly of Au nanoparticles.

film). The impedance of the spiral ITO substrate was 6 $\Omega \cdot cm^2$, which was expected to have no harmonic peak from 0.5 GHz to 3 GHz. The experimental result confirmed this case (Supplementary Information, Fig. S5). However, after the LBL-assembly of gold nanoparticles, the spoof LSP showed an obvious resonance peak in microwave band (Fig. 3a). It is interesting that there was only one resonance peak for the assembled LSP, which is different from that of the bulk LSP spiral. When the number of assembled layers was lower than 20, no obvious resonance signal was observed. For 20 layers, a blunt resonance signal was found at 1.54 GHz. With the number of assembled layers increasing, the resonance peak shifted to 1.68 GHz and became sharp. Seen from the further magnification graph, the amplitude of resonance signal at 1.68 GHz increased with addition of the assembly layers. We further measured the distribution of near field from 0.5 GHz to 3 GHz that was 5 μm above the surface of spoof LSP spiral. At 1.38 GHz and 2.05 GHz, both the electric and the magnetic resonance modes appeared for the bulk copper spoof LSP (Fig. 3c-d). Nevertheless, only the magnetic resonance mode was found for the LBL-assembled spoof LSP at 1.68 GHz (Fig. 3e-f). Thus, the resonance peak in 1.68 GHz corresponded to the magnetic resonance mode for the LBL-assembled spoof LSP.

This phenomenon is greatly interesting and will facilitate the practical application of LSPR in microwave band. Since only the material composition was altered rather than the structure, we employed CST software to simulate the influences from the material upon the LSPR effect. Here, because the spoof LSP was composed of numerous nanoparticles which were uniform and compact, the film was still regarded as macroscopically continuous medium. It has been demonstrated that the electric resonance component of LBL assembled spoof LSPs disappeared, which is significantly different from that of the spoof LSPs by bulk metal. We wondered whether this phenomenon resulted from the material composition. Thus, we simulated the influences from the different materials (Au, Ag, Cu) upon the LSPR effect. Firstly, the different composition and different film thickness were simulated to show the influence upon the LSPR effect. The composition was set as Au, Ag and Cu. The film thickness was set as 300, 600, 900 and 1600 nm (composition: Au). It was found that neither of them had significant influence on the resonance signals, as shown in Supplementary Information, Fig. S6. However, surface impedance was found to significantly influence the LSPR effect with the simulation. The results were shown in Fig. 4a-c (Further magnifications were shown in Supplementary

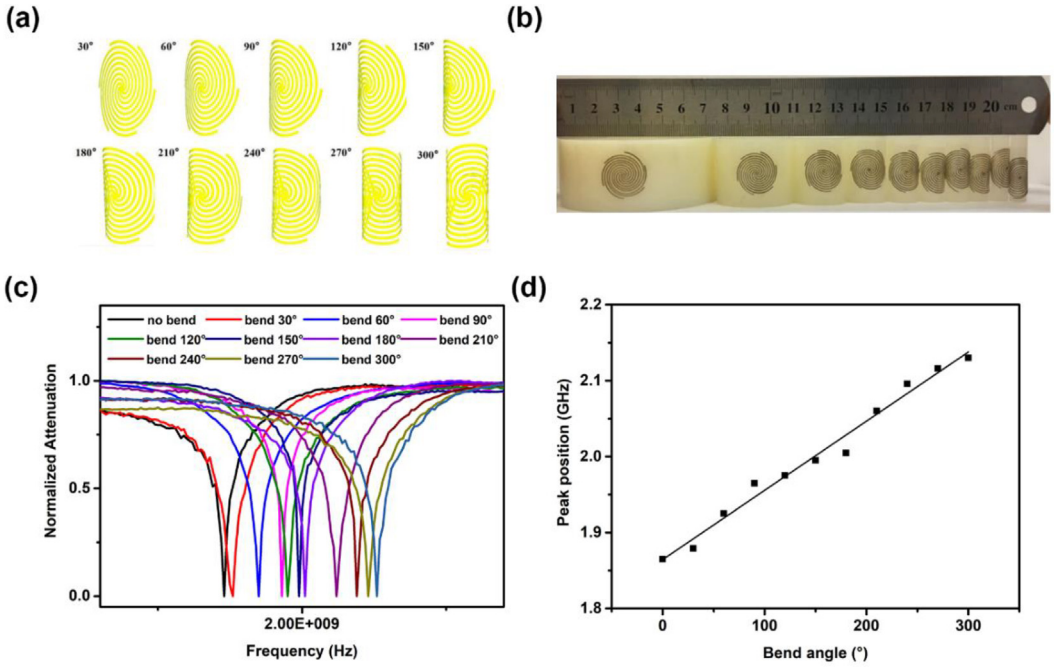

Fig. 5. LSPR performance of the bending spoof LSP by assembly of Au nanoparticles. a) Schematic show of the spoof LSP with different bending angles. b) Photographs of the bending spoof LSPs for experimental measurement. c) Experimental LSPR spectra of the bending spoof LSPs with different angles. d) Linear correlative coefficient between the bending angles and the frequency position of the LSPR.

Information, Fig. S7), where both the electric and the magnetic resonance peaks of LSPR gradually extincted with increase of the surface impedance of the spoof LSP. We measured the surface impedance of the bulk copper spoof LSP and the 50 layer-LBL-assembled spoof LSP from 1 MHz to 3GHz (Fig. 4d). The surface impedance of the LBL-assembled spoof LSP was found larger than that of the bulk copper LSP, and the higher frequency made this case more significant. This case prompted us that the impedance was relative with the disappearance of electric resonance mode in the LBL-assembled spoof LSP spiral but just attribution to the macroscopic conductivity is inadequate to account for this phenomenon. Considering Fig. 2c-j, Supplementary Information, Fig. S3 and Supplementary Information, Fig. S4, the assembled film was composed of clusters of gold nanoparticles. This special microstructure may result in the interesting LSPR effect. Previously, a mixed mechanism of the percolation model and the hopping model was proposed to explain the electroconductibility of such assemblies of nanoparticles. [14] Inside the clusters, the electrons are free because of compact aggregation so that one cluster can be regarded as a conductive ball. Between the clusters, the electrons transport by relying on some weak pathways such as the hopping. Therefore, the collective conductivity becomes low. To further investigate the probable mechanism, COMSOL software was employed to simulate the electromagnetic response of a film that consist of Au clusters when a coming plane electromagnetic wave propagating along. Seen from the electric field response (Fig. 4e) and its magnification for single cluster (Fig. 4f), the electric fields were confined normal to the surfaces of clusters. Thus, the adjacent electric fields will counteract each other so that the electric resonance mode disappeared, which was also confirm by the 2D simulation (Supplementary Information, Fig. S8). However, compared with the electric field, the magnetic field distributed around the surface of clusters (Fig. 4g, h). Because the magnetic force lines must be closed, the magnetic field can still pass through the spoof LSP. Thus, there remained the magnetic resonance mode but the electric resonance mode disappeared due to the counteraction of electric force lines. This mechanism was depicted in Fig. 4i.

One advantage of the spoof LSP by LBL-assembled gold nanoparticles lies in the flexibility, with which relationship between the mechanical strain and the LSPR effect can be investigated. We fixed the flexible spoof LSP spirals onto side wall of nylon cylinders which bottom radius was calculated to guarantee the spoof LSP bent to a certain angle (Fig. 5a). In our experiments, the spoof LSP spirals were bent from 30° to 300° (Fig. 5b) and the corresponding LSPR spectra were shown in Fig. 5c. Interestingly, it was found the LSPR peak gradually shift towards high frequency with increase of the bending angle. The linear correlation coefficient between the LSPR frequency and the bending angle reached 0.9746 (Fig. 5d). The result indicated that the LSPR in microwave band can be modulated by structural deformation of the spoof LSPs. This phenomenon will greatly expand the application of spoof LSPs and deepen understanding of couplings between the LSPR and other actuating variables.

We also experimentally tried sputtering method to fabricate the spoof LSP composed by nanoparticles. It was found the sputtering spoof LSP possessed the similar LSPR behaviours with the LBL-assembled spoof LSP. The results were shown in Supplementary Information, Fig. S9. In morphology, the sputtering method also produced a film of nanoparticles. However, these nanoparticles formed less clusters. The sputtering spoof LSPs also showed single peak in the LSPR spectra and linear correlation with the bending angles. However, the modulated range of LSPR peak by bending angle turned narrowed and the linear correlation coefficient was much smaller.

4. Conclusion

In summary, a novel ultrathin and flexible LSP was constructed by LBL-assembly of gold nanoparticles. After resonance measurements by vector network analyzer, we noticed that the spoof LSP showed an obvious assembly-induced LSPR resonance in microwave band. Simulation and experimental investigations showed that only one obvious harmonic peak in the microwave frequency was observed with the assembled layer increasing compared to that made up of metallic copper and the reason may be due to the high surface impedance. Resonance in optical frequency were also observed and the signal broadened due to the aggregation of gold nanoparticles. Furthermore, the resonance signal of

ultrathin and flexible LBL-assembled spoof LSP with bending angle from 30 to 300 degrees were measured and the shift of the peak position perfectly matches with the bow angle, which is of great sensitivity to its changes of surroundings. Because the electromagnetic field can effectively penetrate human tissue, the novel ultrathin and flexible spoof LSP LBL-assembled by gold nanoparticles with dual-frequency resonance will greatly widen the application of gold nanomaterials-based metamaterial in biomedicine.

Credit author statement

Peng Wang: Writing - Original Draft, Investigation, Validation. Xiaopeng Shen, Haoshen Wang: Software, Data Curation. Haochi zhang, Ou Xu and Peihang He: Validation, Methodology. Siyu Ma and Zhaobin Guo: Writing - Review & Editing. Qing Jiang: Funding acquisition. Ning Gu and Jianfei Sun: Conceptualization, Funding acquisition and Project administration.

Declaration of Competing Interest

None.

Acknowledgments

This work was financially supported by grants from National Key Research and Development Program of China (2017YFA0104301) and National Natural Science Foundation of China (NSFC, 81802135). J. Sun greatly appreciated Prof. N. A. Kotov in University of Michigan for learning the LBL assembly technology and Prof. Tiejun Cui in Southeast University for providing an opportunity to know the spoof LSPs. Prof. Yijun Feng and Dr. Ke Chen were greatly appreciated for helps in simulation discussion.Peng wang and Xiaopeng Shen contributed equally to this work.

Appendix A. Supplementary data

Supplementary data to this article can be found online at https://doi.org/10.1016/j.matdes.2021.109622.

References

[1] A. Gelle, T. Jin, L.D. Garza, G.D. Price, A. Moores, Applications of plasmon-enhanced nanocatalysis to organic transformations, Chem. Rev. 120 (2019) 986–1041.
[2] Y. Chen, W. Chang, C. Li, Y. Chiu, C. Huang, C. Lin, Direct synthesis of monolayer gold nanoparticles on epoxy based photoresist by photoreduction and application to surface-enhanced Raman sensing, Mater. Des. 197 (2021) 109211.
[3] V. Amendola, R. Pilot, M. Frasconi, M. Onofrio, A. Maria, Surface plasmon resonance in gold nanoparticles: a review, J. Phys. Condens. Matter 29 (2017) 203002.
[4] W. Zhang, Z. Jiang, L. Hao, G. Lu, Y. Ning, C. Lu, Z. Xu, Three-dimensional ordered macroporous nano-architecture and its enhancing effects on raman detection sensitivity for eosin y molecules, Mater. Des. 119 (2017) 456–463.
[5] H.R. Culver, M.E. Wechsler, N.A. Peppas, Z. Tavasoli, Label-free detection of tear biomarkers using hydrogel-coated gold Nanoshells in a localized surface plasmon resonance-based biosensor, ACS Nano 12 (2018) 9342–9354.
[6] C. Kuppe, K. Rusimova, L. Ohnoutek, D. Slavov, V.K. Valev, Hot in Plasmonics: Temperature-Related Concepts and Applications of Metal Nanostructures, Adv. Opt. Mater. 8 (2020) 1901166.
[7] R. Li, M.R. Bourgeois, C. Cherqui, J. Guan, D.Q. Wang, J.T. Hu, R.D. Schaller, G.C. Schatz, T.W. Odom, Hierarchical hybridization in plasmonic honeycomb lattices, Nano Lett. 19 (2019) 6435–6441.
[8] M. Kataria, K. Yadav, A. Nain, H.I. Lin, H.W. Hu, C.R.P. Inbaraj, T.J. Chang, Y.M. Liao, H.Y. Cheng, K.H. Lin, H.T. Chang, F.G. Tseng, W.H. Wang, Y.F. Chen, Self-sufficient and highly efficient gold sandwich upconversion nanocomposite lasers for stretchable and bio-applications, ACS Appl. Mater. Interfaces 12 (2020) 19840–19854.
[9] M.G. Gong, M.H. Alamri, D. Ewing, S.M. Sadeghi, J.Z. Wu, Localized surface plasmon resonance enhanced light absorption in AuCu/CsPbCl3 core/shell nanocrystals, Adv. Mater. 12 (2020) 19840–19854.
[10] B. Sun, Y. Yu, Double toroidal spoof localized surface plasmon resonance excited by two types of coupling mechanisms, Opt. Lett. 44 (2019) 1444–1447.
[11] W.X. Tang, H.C. Zhang, H.F. Ma, W.X. Jiang, T.J. Cui, Concept, theory, design, and applications of spoof surface plasmon polaritons at microwave frequencies, Adv. Opt. Mater. 7 (2019) 1800421.
[12] H.J. Lezec, A. Degiron, E. Devaux, R.A. Linke, L.M. Moreno, F.J.G. Vidal, T.W. Ebbesen, Beaming light from a subwavelength aperture, Science 297 (2002) 820–822.
[13] C.R. Williams, S.R. Andrews, S.A. Maier, A.F. Dominguez, L.M. Moreno, F.J.G. Vidal, Highly confined guiding of terahertz surface plasmon polaritons on structured metal surfaces, Nat. Photonics 2 (2008) 175–179.
[14] X. Shen, T.J. Cui, Ultrathin plasmonic metamaterial for spoof localized surface plasmons, Laser Photonics Rev. 8 (2014) 137–145.
[15] H. Zhang, L. Feng, Y. Liang, T. Xu, An ultra-flexible plasmonic metamaterial film for efficient omnidirectional and broadband optical absorption, Nanoscale. 11 (2019) 437–443.
[16] P. Wang, M.E. Nasir, A.V. Krasavin, W. Dickson, A.V. Zayats, Plasmonic metamaterials for nanochemistry and sensing, Acc. Chem. Res. 52 (2019) 3018–3028.
[17] W. Wu, W. Hu, G. Qian, H.T. Liao, X.Y. Xu, F. Berto, Mechanical design and multifunctional applications of chiral mechanical metamaterials: a review, Mater. Des. 180 (2019) 107950.
[18] S. Yu, A.J. Wilson, J. Heo, P.K. Jain, Plasmonic control of multi-Electron transfer and C–C coupling in visible-light-driven CO_2 reduction on au nanoparticles, Nano Lett. 18 (2018) 2189–2194.
[19] M. Sharifi, S.H. Hosseinali, R.H. Alizadeh, A. Hasan, M. Falahati, Plasmonic and chiroplasmonic nanobiosensors based on gold nanoparticles, Talanta 212 (2020) 120782.
[20] M.P. Singh, G.F. Strouse, Involvement of the LSPR spectral overlap for energy transfer between a dye and Au nanoparticle, J. Am. Chem. Soc. 132 (2010) 9383–9391.
[21] K. Rusimova, D. Slavov, F. Pradauxcaggiano, J.T. Collins, S.N. Gordeev, D.R. Carbery, W.J. Wadsworth, P.J. Mosley, V.K. Valev, Atomic dispensers for thermoplasmonic control of alkali vapor pressure in quantum optical applications, Nat. Commun. 10 (2019) 2328.
[22] A.J. Senesi, D.J. Eichelsdoerfer, R.J. Macfarlane, M.R. Jones, E. Auyeung, B. Lee, C.A. Mirkin, Stepwise evolution of DNA-programmable nanoparticle superlattices, Angewandte Chemie-International Edition 26 (2013) 6624–6628.
[23] Y. Chen, H. Liu, H. Yin, Q. Zhu, N. Gu, Hierarchical fabrication of plasmonic superlattice membrane by aspect-ratio controllable nanobricks for label-free protein detection, Front. Chem. 8 (2020) 307.
[24] X. Wu, J. Chen, L. Xie, J. Li, J. Shi, S.P. Luo, X.X. Zhao, K. Deng, D.S. He, J.Q. He, J. Luo, Z.W. Wang, Z.W. Quan, Directing gold nanoparticles into free-standing honeycomb-like ordered Mesoporous superstructures, Small 15 (2019) 1901304.
[25] M.B. Ross, J.C. Ku, V.M. Vaccarezza, G.C. Schatz, C.A. Mirkin, Nanoscale form dictates mesoscale function in plasmonic DNA–nanoparticle superlattices, Nat. Nanotechnol. 10 (2015) 453–458.
[26] Y. Kim, J. Zhu, B. Yeom, M.D. Prima, X. Su, J.G. Kim, S.J. Yoo, C. Uher, N.A. Kotov, Stretchable nanoparticle conductors with self-organized conductive pathways, Nature. 500 (2013) 59–63.
[27] P. Wang, J. Sun, Z. Lou, F.G. Fan, K. Hu, Y. Sun, N. Gu, Assembly-induced thermogenesis of gold nanoparticles in the presence of alternating magnetic field for controllable drug release of hydrogel, Adv. Mater. 28 (2016) 10801–10808.
[28] Y. Zhang, P. Wang, H. Mao, Y. Zhang, L. Zheng, P. Yu, Z. Guo, L. Li, Q. Jiang, PEGylated gold nanoparticles promote osteogenic differentiation in in vitro and in vivo systems, Mater. Des. 197 (2021) 109231.
[29] A. Pors, E. Moreno, L. Martinmoreno, J.B. Pendry, F.J.G. Vidal, Localized spoof plasmons arise while texturing closed surfaces, Phys. Rev. Lett. 108 (2012) 223905.
[30] Z. Liao, X. Shen, B.C. Pan, J. Zhao, Y. Luo, T.J. Cui, Combined system for efficient excitation and capture of LSP resonances and flexible control of SPP transmissions, ACS Photonics 2 (2015) 738–743.
[31] Z. Liao, A.I. Fernández-Dominguez, J.J. Zhang, S.A. Maier, T.J. Cui, Y. Luo, Homogenous metamaterial description of localized spoof plasmons in spiral geometries, ACS Photonics 10 (2016) (2016) 1768–1775.
[32] J.A. Lock, G. Gouesbet, Generalized lorenz–mie theory and applications, J. Quant. Spectrosc. Radiat. Transf. 110 (1994) 800–807.
[33] H. Zhang, J. Shih, J. Zhu, N.A. Kotov, Layered nanocomposites from gold nanoparticles for neural prosthetic devices, Nano Lett. 7 (2012) 3391–3398.
[34] J. Lipton, G.M. Weng, J.A. Rhr, H. Wang, A.D. Taylor, Layer-by-layer assembly of two-dimensional materials: meticulous control on the nanoscale, Matter. 5 (2020) 1148–1165.
[35] T. Liu, Y. Wang, W. Zhong, B.Y. Li, K. Mequanint, G.X. Luo, Biomedical applications of layer-by-layer self-assembly for cell encapsulation: current status and future perspectives, Adv. Healthc. Mater. 1 (2019) 1800939.
[36] D. Melnikau, R. Esteban, D. Savateeva, A.S. Iglesias, M. Grzelczak, M.K. Schmidt, L.M. Marzan, J. Aizpurua, Y.P. Rakovich, Rabi splitting in photoluminescence spectra of hybrid systems of gold nanorods and J-aggregates, J. Phys. Chem. C 7 (2016) 354–362.
[37] N.T. Fofang, T. Park, O. Neumann, N.A. Mirin, N. Peter, N.J. Halas, Plexcitonic nanoparticles: plasmon-exciton coupling in nanoshell-J-aggregate complexes, Nano Lett. 8 (2008) 3481–3487.